Monthly calibration of Hargreaves–Samani equation using remote sensing and topoclimatology in central-southern Chile

Article *in* International Journal of Remote Sensing · May 2017

DOI: 10.1080/01431161.2017.1323287

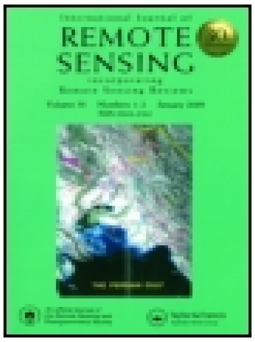

Taylor & Francis
Taylor & Francis Group

International Journal of Remote Sensing

ISSN: 0143-1161 (Print) 1366-5901 (Online) Journal homepage: http://www.tandfonline.com/loi/tres20

Monthly calibration of Hargreaves–Samani equation using remote sensing and topoclimatology in central-southern Chile

Luis Morales-Salinas, Samuel Ortega-Farías, Camilo Riveros-Burgos, José Neira-Román, Marcos Carrasco-Benavides & Rafael López-Olivari

To cite this article: Luis Morales-Salinas, Samuel Ortega-Farías, Camilo Riveros-Burgos, José Neira-Román, Marcos Carrasco-Benavides & Rafael López-Olivari (2017): Monthly calibration of Hargreaves–Samani equation using remote sensing and topoclimatology in central-southern Chile, International Journal of Remote Sensing, DOI: 10.1080/01431161.2017.1323287

To link to this article: http://dx.doi.org/10.1080/01431161.2017.1323287

Published online: 26 May 2017.

INTERNATIONAL JOURNAL OF REMOTE SENSING, 2017
https://doi.org/10.1080/01431161.2017.1323287

Monthly calibration of Hargreaves–Samani equation using remote sensing and topoclimatology in central-southern Chile

Luis Morales-Salinas[a], Samuel Ortega-Farías[b,c], Camilo Riveros-Burgos[b,c], José Neira-Román[d,e], Marcos Carrasco-Benavides[f] and Rafael López-Olivari[g]

[a]Laboratory for Research in Environmental Sciences (LARES), Faculty of Agricultural Sciences, University of Chile, Santiago, Chile; [b]Research and Extension Center for Irrigation and Agroclimatology (CITRA), University of Talca, Talca, Chile; [c]Research Program on Adaptation of Agriculture to Climate Change (PIEI A2C2), University of Talca, Talca, Chile; [d]Centro de Estudios Avanzados en Fruticultura (CEAF) Conicyt-Regional, Rengo, Chile; [e]Departamento de Ciencias Ambientales y Recursos Naturales Renovables, Facultad de Ciencias Agronómicas, Universidad de Chile, Santiago, Chile; [f]Department of Agricultural Sciences, Universidad Católica del Maule, Curicó, Chile; [g]Instituto de Investigaciones Agropecuarias, INIA, Temuco, Chile

ABSTRACT

Reference evapotranspiration (ET_o) has a key role in irrigation scheduling. In this sense, the Hargreaves–Samani equation (HS) is a reliable and widely used method to estimate ET_o. The HS equation just requires temperature and solar radiation data, making it a suitable method for places that lack of wind speed and relative humidity information. However, literature shows that a local calibration of its empiric parameter is needed for its complete application. This work shows a calibration for the Maule region in central-southern Chile. For this purpose, the Penman–Monteith equation from FAO-56 (PM) was considered as a reference, using a network of 400 meteorological stations between the 32° and 39° of south latitude for the 1973–2011 period. The calibration was based on the computation of the ratio of ET_o calculated by HS and PM and the spatial behaviour of input variables and parameters. The spatial distribution was done by geographical weighted regression and ordinary Kriging with a linear variogram, assisted by a digital elevation model from the Shuttle Radar Topography Mission and surface reflectances from Moderate Resolution Imaging Spectroradiometer. The process of calibration was validated with daily data through all months, with comparative errors of 5% against PM.

ARTICLE HISTORY
Received 9 August 2016
Accepted 20 April 2017

1. Introduction

Currently, Chilean agriculture is facing challenges to develop and apply sustainable practices to optimize the use of water for irrigation. These requirements take major value considering the cyclical occurrence of 'La Niña,' the cold phase of the 'El Niño-Southern Oscillation,' which has significantly reduced water supply (precipitation) for agriculture (Garreaud 2009; Meza 2005). Besides the fact that 70% of the world

CONTACT Samuel Ortega-Farías sortega@utalca.cl Research and Extension Center for Irrigation and Agroclimatology (CITRA), University of Talca, Talca, Chile

consumption of water is associated with agriculture, this value may increase to 90% in arid zones in Chile (Larraín 2006).

To deal with both optimization and efficient water use for irrigation, it is necessary to handle methodologies to estimate crops' water consumption. In this sense, reference evapotranspiration (ET_o) has taken an essential role, because it accounts for climatic effects on crop water demands. It means that ET_o plays a key role in the planning of an appropriate irrigation scheduling (Cammalleri et al. 2013; Valipour and Eslamian 2014; Valipour 2015c). ET_o may be calculated using complex equations with a great number of input variables as well as simpler models, which just need few meteorological variables as input (Hargreaves and Samani 1985; Valipour 2015a; 2015b).

The most used model to estimate ET_o is the Penman–Monteith equation (PM) proposed by the Food and Agriculture Organization of the United Nations (FAO) (Allen et al. 1998). This approach defines ET_o as the water consumption of a reference crop growing in optimal conditions. PM model is the most used and validated method under different climatic conditions since it includes physical, aerodynamical, and physiological effects. Thereby, this model has been taken as the basis of validation for simpler models developed in order to manage the typical limited meteorological information (Martinez and Thepadia 2009; Thepadia and Martinez 2012; Trajkovic and Kolakovic 2009; Valipour 2015d; 2015e).

Meteorological time series always have problems and limitations associated to data continuity and poor geographic distribution of meteorological stations (Hargreaves and Allen 2003; Hargreaves and Samani 1985; Trajkovic and Kolakovic 2009). Therefore, models with low input variables are needed. One of the simplest models corresponds to the Hargreaves–Samani (HS) equation, which also was recommended by FAO (Allen et al. 1998). The HS model is a good choice when there is not enough information to use PM because it just uses daily extreme temperatures and solar radiation. The HS equation presents a good fit and reliable estimation of ET_o considering different time steps (monthly, weekly, and daily). However, it must be calibrated to local conditions (Droogers and Allen 2002; Hargreaves and Allen 2003; Hargreaves 1989; Valipour 2014; Valipour 2015f). Several researchers have calibrated the HS model using the PM approach in different parts of the world. The HS equation has already been used in Chile, from Chaca Valley in the north (Torres Hernández and Vásquez Vásquez 2013) to Osorno in the southern region (Rivano and Jara 2005), but it remains uncalibrated for the conditions in Maule region (MR).

The performance of HS equation depends directly on daily temperature range (ΔT), which may be influenced by distance inland, altitude, latitude, topography, or proximity to a large body of water (Mendicino and Senatore 2013). Therefore, in order to develop an adequate calibration, it is necessary to prove the influence of physiography on HS equation. To carry it out, remote sensing data were used as the basis, since they allow the consideration of the ET spatial continuity phenomena, and they provide the opportunity to get periodical information from extensive areas (Ambast, Keshari, and Gosain 2002; Sánchez and Chuvieco 2000). Consequently, the objective of this study was to calibrate the parameters of the HS equation, taking into account for the spatial variability of temperatures in the MR.

2. Materials and methods

2.1. *Study area*

The study area corresponds to the MR in the central-southern part of Chile (Figure 1). It is characterized by a warm temperate climate with a four-to-five-month dry season. The thermal regime is defined by hot and dry summers with cold winters. Maximum mean temperature is 26.9°C in January, minimum mean temperature is 3.9°C in July, and annual mean rainfall is 1005 mm (Uribe et al. 2012).

2.2. *Meteorological data*

Meteorological information was obtained from stations from both Chile's General Water Department (DGA) and Chilean Meteorological Department (DMC). Additional information was considered from historical time series from Agroclimatic map of Chile (Novoa et al. 1989) reaching 404 stations from O'Higgins (OR), MR and Bío-Bío (BBR) regions (Figure 2).

Stations belonging to the MR were 136, while the remaining 238 were from the OR and BBR. The last ones were needed to ensure continuity on estimation models of spatial distribution for studied variables (topoclimatic models). Variables extracted from every station were number of recording years, geographical location (latitude and longitude), altitude, slope, exposition, precipitation (PP), monthly mean maximum and minimum temperature (T_{Max} and T_{Min}), monthly mean temperature (T_{Mean}), monthly mean relative humidity (RH), monthly accumulated solar radiation (SR), cloudiness (CDS), pan evapotranspiration (pET_o), and wind speed (WS). Only stations with at least 10 years of continuous recording were used, and geographical location was saved with the geographical coordinate system under the World Geodetic System of 1984 (WGS84) reference system. For the selected weather stations that met this requirement, the average monthly data were reviewed carefully and subjected to quality and integrity controls (Allen 1996; Estévez, Gavilán, and García-Marín 2011). The procedure undergoes a check of missing and out of range data (more than two

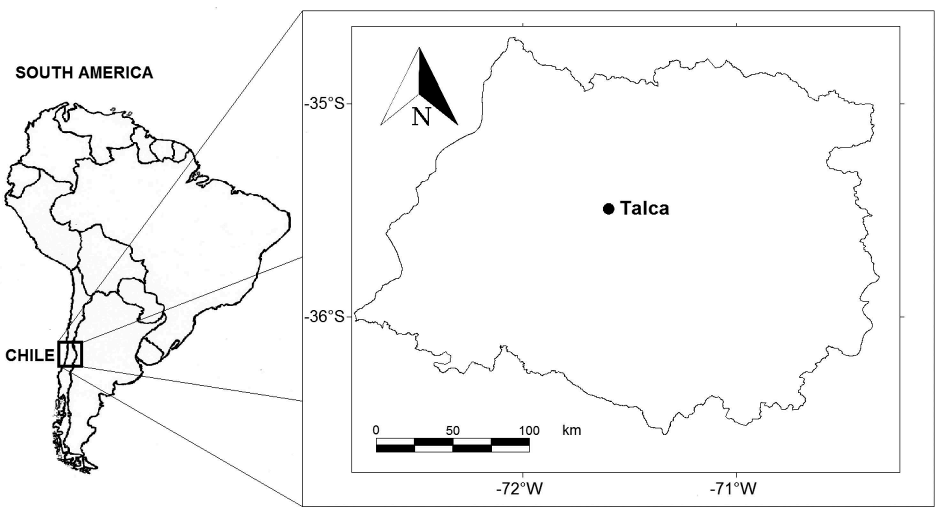

Figure 1. Geographical location of study area.

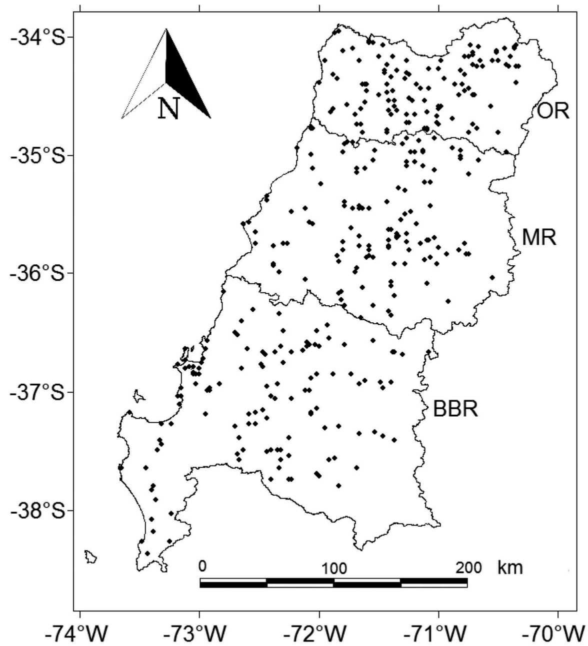

Figure 2. Geographical distibution of meteorological stations considered in the study. OR; MR, and BBR.

times the standard deviation for that month), which were replaced by −9999. Subsequently, the data were estimated using an ordinary Kriging with linear variogram for missing and anomalous months. Time series limitation is shown in Table 1.

2.3. *Satellite data*

A digital elevation model (DEM) was used to characterize the spatial dependence of climatological variables and field altitude. It was obtained from Global Land Cover Facility (http://www.landcover.org/). The product corresponded to the fourth version of Shuttle Radar Topographic Mission (SRTM4), and it accounted with a 90-m spatial resolution. Terra-Moderate Resolution Imaging Spectroradiometer (Terra-MODIS) imagery was also considered. It consisted of surface reflectance images composed by 8 days with a 250-m spatial resolution (MOD09Q1 product) between the years 2002–2012. Each MOD09Q1 pixel was selected on the basis of high observation coverage, low view angle, the absence of clouds or cloud shadow, and aerosol loading (Vermote and Kotchenova 2011). This product was used to calculate the monthly mean normalized difference vegetation index (NDVI) (Tucker 1979). Both MOD09Q1 and SRTM4 were trimmed to the study area (Figure 1) and then projected to WGS84.

2.4. *HS model*

The HS model estimates ET_o as follows:

Table 1. Number of stations by recorded variables in studied area.

Region	Precipitation	Solar radiation	Reference evapotranspiration	Relative humidity	Cloudiness	Maximum temperature	Minimum temperature	Mean temperature	Wind speed
OR, MR and BBR	314	34	38	61	36	81	78	62	11
MR	88	10	13	14	11	23	22	12	2

$$\mathrm{ET_{oHS}} = K_{\mathrm{HS}} R_{\mathrm{s}} (T_{\mathrm{a}} + 17.78), \tag{1}$$

where R_s is solar radiation (mm day^{-1}), K_{HS} is an empiric parameter (dimensionless), and T_a is the daily mean air temperature (°C). When there is no solar radiation data, it is possible to use the clearness index (CI) to estimate missing information. Hargreaves and Samani (1982) recommended a simple way to estimate it as a function of temperature:

$$\mathrm{CI} = \frac{R_{\mathrm{s}}}{R_{\mathrm{a}}} = K_{\mathrm{T}} (T_{\mathrm{Max}} - T_{\mathrm{Min}})^{0.5}, \tag{2}$$

where R_a is extra-terrestrial radiation (mm day^{-1}), which was calculated as a function of the distance from the Sun to Earth, the mean distance Sun–Earth, latitude, solar declination, and solar angle at sunrise (Iqbal 1983; Allen et al. 1998; Meza and Varas 2000). K_T is an empiric parameter (dimensionless), and T_{Max} and T_{Min} are daily maximum and minimum air temperatures (°C), respectively. Hargreaves and Samani (1985) derived a simplified equation based on Equations (1) and (2):

$$\mathrm{ET_{oHS}} = K_{\mathrm{HS}} K_{\mathrm{T}} (T_{\mathrm{a}} + 17.78)(T_{\mathrm{Max}} - T_{\mathrm{Min}})^{0.5} R_{\mathrm{a}}, \tag{3}$$

where K_{HS} and K_T usually take a value of 0.0135 and 0.17, respectively (Shahidian et al. 2014). K_{HS} and K_T were recalculated monthly for every station considered in this study.

2.5. *Calibration*

2.5.1. *Topoclimatology*

To study spatial variation of ET_o using the HS model, a spatial characterization of input variables such as R_a, R_s, T_{Max}, and T_{Min} was necessary. This task was carried out studying with topoclimatology the effect of terrain on climate. Therefore, climatic data were estimated through spatial modelling of parametric instability phenomena (Draper and Smith 1981; Tomislav et al. 2009). This analysis considered the spatial variation of linear regression parameters (Morales-Salinas 1997; Morales-Salinas et al. 2009) using weighted least squares, which is a correlation function between every point and the remaining points using a weighted distance. The model proposed corresponds to the geographical weighted regression (GWR) (Brunsdon, Fotheringham, and Charlton 1996):

$$y_i = a_0(u_i, v_i) + \sum_k a_k(u_i, v_i) x_{i,k} + \varepsilon_i, \tag{4}$$

where (u_i,v_i) are the ith point coordinates, y_i is the response variable, $x_{i,k}$ is the kth independent variable at ith point, a_k is the kth regression parameter, and ε_i is the residual at ith point. The R_a and R_s were estimated as a function of the altitude (DEM), while the T_{Max} and T_{Min} were described by the altitude (DEM) and the vegetal cover through the NDVI. It was considered because the vegetation plays a key role in the complex interactions between the land surface and the atmosphere. Moreover, meteorological and climatological conditions both impact and are influenced by vegetation distribution and dynamics (Hong, Lakshmi, and Small 2007). Then, the main advantage of using the MOD09Q1 is that it allows taking into account for quantitative vegetation characteristics (Westerhoff 2015).

The second part in the variable spatialization process consisted in the use of ordinary Kriging model, with a linear semi-variogram (Martínez-Cob 1996; Miranda-Salas and Condal 2003; Vicente Serrano, Sánchez, and Cuadrat 2003).

2.5.2. *Parameter estimation*

The K_T calibration was obtained monthly from Equation (2), based on input variables modelled by topoclimatology. Subsequently, a descriptive analysis was done to know its annual variability. In order to calibrate the original K_{HS} parameter using monthly data, the PM model was used as reference as follows:

$$X = \frac{(\mathrm{ET})_{\mathrm{oPM}}}{(\mathrm{ET})_{\mathrm{oHS}}}, \tag{5}$$

where X is the ratio between the $\mathrm{ET_o}$ computed by PM equation ($\mathrm{ET_{oPM}}$) and HS model ($\mathrm{ET_{oHS}}$). Then the HS equation was corrected as (Ghamarnia et al. 2011)

$$K_{(\mathrm{HS\text{-}C})} = 0.0135X, \tag{6}$$

where $K_{\mathrm{HS\text{-}C}}$ is the monthly corrected parameter for each station. The $\mathrm{ET_{oPM}}$ is given by (Allen et al. 1998)

$$\mathrm{ET_{oPM}} = \frac{0.408\Delta(R_n - G) + \gamma\left(\frac{900}{T+273}\right)u_2(e_s - e_a)}{\Delta + \gamma(1 + 0.34u_2)} \tag{7}$$

where R_n is net radiation over reference crop surface (MJ m^{-2} day^{-1}), G is soil heat flux (MJ m^{-2} day^{-1}), T is daily mean air temperature ($^{\circ}$C) at 2 m above ground, u_2 is daily mean wind speed at 2 m above ground (m s^{-1}), e_s is saturated vapour pressure (kPa), e_a is actual vapour pressure (kPa), Δ is the slope of the vapour pressure versus temperature curve (kPa $^{\circ}$C^{-1}), and γ is the psychrometric constant (kPa $^{\circ}$C^{-1}).

In order to find areas with similar spatial and temporal performance, a classification of homogeneous zones was done. This process is based on physical aspects that are shown in function of their main characteristics and temporal behaviour (Morales-Salinas et al. 2006; Qiyao, Jingming, and Baopu 1991). The use of this process was through K-means analysis. This method uses Euclidean distance as a likelihood measure for an automatic classification in previously unknown homogeneous groups (Pérez 2004):

$$E_d = \sqrt{\sum_{i=1}^{p} (x_{ri} - x_{si})^2} \tag{8}$$

where E_d is the euclidean distance, x_{ri} is one of studied variables from 'r_i' object, x_{si} is the same variable from 's_i' object, and p is number of objects to classify. The 'objects' are the image's pixels, and properties associated to that element were stored in a vectorial format.

2.6. *Validation*

After the calibration process, daily $\mathrm{ET_o}$ was calculated with the mean monthly HS equation proposed. In order to apply it on a daily basis, the proposed mean K_{HS} was interpolated using a cubic spline algorithm to achieve a monotonous transition between consecutive months (Higham 1992).Then, it was compared against daily ET_{oPM}. The weather stations used in the validation were different than those used in calibration. These data belong to the 'Instituto de Investigaciones Agropecuarias' (INIA, Chile), Global Surface Summary of Day from the National Oceanic and Atmospheric Administration (NOAA), and Research and Extension Center for Irrigation and Agroclimatology (CITRA).

2.7. *Statistical analysis*

Topoclimatic models based on GWR were evaluated with the Akaike information criterion (AIC), which is useful to compare at least two models with the same dependent and independent fixed variables (Sakamoto, Ishiguro, and Kitagawa 1986; Burnham and Anderson 1998). The AIC was calculated as follows:

$$\mathrm{AIC} = 2k + N \ln\left(\frac{\sum_{N}^{i=1}(O_i - E_i)^2}{N}\right). \tag{9}$$

Results from general analysis were based on daily comparison between HSc and PM. Deviation of estimation was analysed with the difference between observed and estimated values (BIAS), mean bias error (MBE), and root mean square error (RMSE). In order to quantify the contribution of calibration, a linear regression analysis was done calculating the slope homogeneity between HS and HSc against PM (Rawlings, Pantula, and Dickey 1998). Furthermore, Model Efficiency Index (Ef) was also calculated as follows:

$$\mathrm{BIAS} = O_i - E_i, \tag{10}$$

$$\mathrm{MBE} = \frac{1}{N}\sum_{i=1}^{N} O_i - E_i, \tag{11}$$

$$\mathrm{MABE} = \frac{1}{N}\sum_{i=1}^{N} |O_i - E_i|, \tag{12}$$

$$\mathrm{RMSE} = \sqrt{\frac{1}{N}\sum_{i=1}^{N}(O_i - E_i)^2}, \tag{13}$$

$$\mathrm{Ef} = 1 - \frac{\sum_{i=1}^{N}(O_i - E_i)^2}{\sum_{i=1}^{N}(O_i - \bar{O})^2}, \tag{14}$$

where N is the number of observations, O is observed data, E is estimated data, and $\bar{O}$ is the mean observed data.

Table 2. Average coefficients of GWR for temperatures (°C) and solar radiation (MJ m^2 day^{-1}) in MR.

Variable	Offset	Altitude	NDVI	RMSE	Ef	R^2(%)	Significance
Mean temperature of January (TME)	20.7	0.00035	−0.12	0.90	0.87	87.2	**
Mean temperature of July (TMJ)	8.9	−0.02513	0.51	0.70	0.89	89.8	**
Minimum temperature of January (TNE)	12.9	0.00077	−0.59	0.70	0.89	90.0	**
Minimum temperature of July (TNJ)	4.2	−0.00305	0.57	0.70	0.89	93.1	**
Maximum temperature of January (TXE)	28.2	0.00656	0.48	0.70	0.89	87.6	**
Maximum temperature of July (TXJ)	13.6	−0.00094	0.54	0.70	0.89	87.7	**
Solar radiation of January (RSE)	27.3	0.01346	–	0.44	0.91	93.0	**
Solar radiation of July (RSJ)	7.6	0.00334	–	0.10	0.98	98.0	**

RMSE units correspond to °C or MJ m^2 day^{-1}, depending on which variable is observed.
The ** is a high statistical significance ($p < 0.01$).

3. Results

3.1. *Topoclimatology*

The Ef for estimated variables ranged between 0.87 and 0.98; additionally determination coefficient (R^2) values showed that the model explained the variability between 87.2% and 98.0% (Table 2). These results exposed a reasonable spatialization of climatological

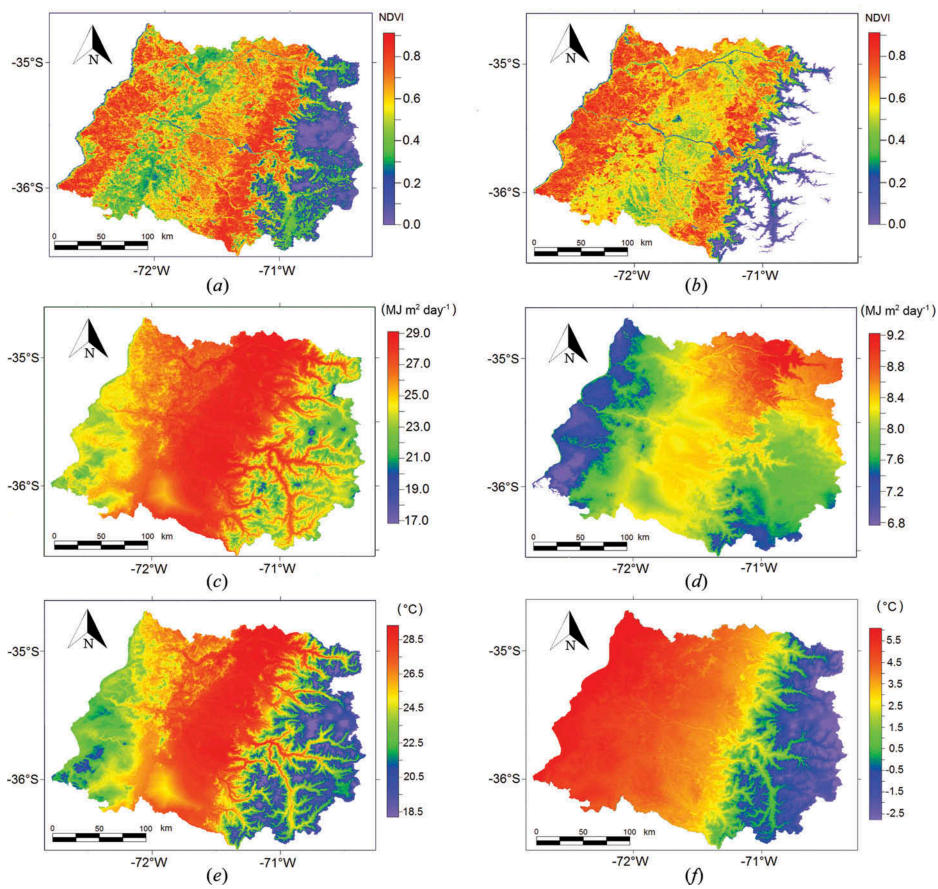

Figure 3. Extreme values of NVDI and estimated spatial distribution of temperatures and solar radiation. Mean NDVI of January (*a*) and July (*b*). Mean solar radiation of January (*c*) and July (*d*). Maximum temperature of January (*e*) and minimum temperature of July (*f*).

variables in function of DEM and NDVI, taking into account for the spatial dependence of linear regression coefficients. Figure 3 shows input variables used in modelling (DEM and NDVI) and three estimated variables such T_{Max}, T_{Min}, and SR. Also, the obtained GWR coefficients, such as the Offset ($\hat{a}_0$), Altitude ($\hat{a}_1$), and NDVI ($\hat{a}_2$) were statistically significant for all estimated variables, and their statistics are presented in Table 2 for main temperatures and solar radiation.

3.2. *Parameter estimation*

Estimated K_T values showed a spatial homogeneity despite the extensive area, which made it possible to estimate solar radiation from monthly mean values of this parameter (Table 3). Nevertheless, different values have been reported in central Chile (Aburto Schweitzer 2007; Castillo and Santibañez 1981; Meza and Varas 2000). K_T values were around 0.154, which allowed a mean monthly estimation of solar radiation with error values less than 5%. Monthly estimated data contrast with values obtained by Raziei and Pereira (2013) for stations situated in the semi-arid to hyper-arid climates of central, southern, and eastern Iran, which ranged between 0.14 and 0.20.

With respect to K_{HS} estimation, stratification was observed from north to south and from the coast to the Andes Mountains. Values from stations (data not shown) ranged in the coast between 0.011 in summer and 0.0079 in winter. Values for the central valley were between 0.012 in summer and 0.0083 in winter. Then, like Heydari and Heydari (2013) found in central Iran (semi-arid and arid conditions), K_{HS} values in the warm and dry months (December, January and February) are higher than those in the cold and rainy months (June, July and August). Table 4 is summarizing K_{HS} estimation based on homogeneous zones (clusters) obtained from K-means analysis.

Clusters showed a length-wise stratification from Pacific Ocean to Andes Mountains, which was present throughout all months (Figure 4). This feature left the physiography effect on climatological variables exposed. Then, coast cluster was based on coastal and internal rain-fed areas, delimited by Coastal Mountains to the east. The valley cluster was located between Coastal and Andes Mountains, corresponding to central valley. Meanwhile, the mountain cluster was the Andes Mountain area. The lowest monthly mean value was 0.00881, obtained for the coast cluster in June, while the highest monthly mean value was 0.02060 for the mountains cluster in June and July. The last

Table 3. Monthly mean estimated values of K_T (Dimensionless).

Month	K_T
January	0.151 ± 0.002379
February	0.152 ± 0.002288
March	0.154 ± 0.002405
April	0.157 ± 0.002280
May	0.161 ± 0.002220
June	0.162 ± 0.002198
July	0.153 ± 0.002163
August	0.157 ± 0.002250
September	0.153 ± 0.002294
October	0.151 ± 0.002342
November	0.150 ± 0.002377
December	0.151 ± 0.002383
Annual	0.154 ± 0.002297

Table 4. Monthly mean estimated values of K_{HS} (dimensionless).

Month	Coast	Valley	Mountains
January	0.01177 ± 0.000234	0.01247 ± 0.000331	0.01355 ± 0.000285
February	0.01214 ± 0.000250	0.01296 ± 0.000407	0.01431 ± 0.000352
March	0.01198 ± 0.000325	0.01316 ± 0.000621	0.01523 ± 0.000528
April	0.01152 ± 0.000455	0.01342 ± 0.001052	0.01690 ± 0.000896
May	0.01044 ± 0.000656	0.01350 ± 0.001784	0.01937 ± 0.001504
June	0.00810 ± 0.000789	0.01273 ± 0.002387	0.02060 ± 0.002036
July	0.00810 ± 0.000789	0.01273 ± 0.002387	0.02060 ± 0.002036
August	0.00964 ± 0.000580	0.01241 ± 0.001681	0.01797 ± 0.001445
September	0.01062 ± 0.000404	0.01237 ± 0.001027	0.01579 ± 0.000886
October	0.01126 ± 0.000295	0.01239 ± 0.000624	0.01447 ± 0.000546
November	0.01168 ± 0.000243	0.01248 ± 0.000412	0.01386 ± 0.000371
December	0.01168 ± 0.000243	0.01248 ± 0.000412	0.01386 ± 0.000371
Annual	0.01086 ± 0.000435	0.01276 ± 0.001093	0.01638 ± 0.000935

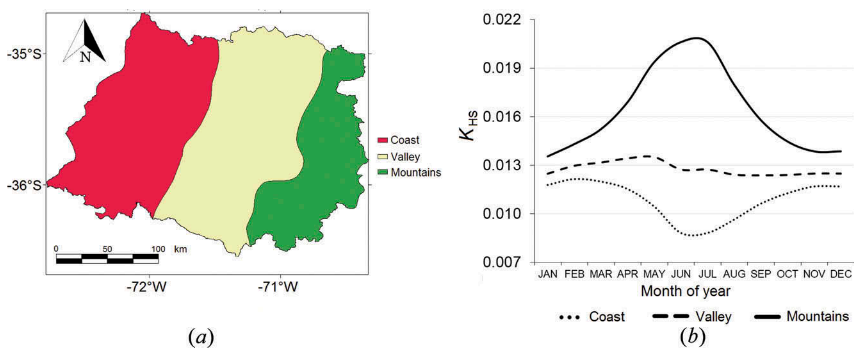

Figure 4. Characterization of K_{HS} clusters in study area. Distribution in the region (*a*) and monthly evolution (*b*).

value probably was obtained due to the complex conditions and the interaction of vegetation and snow in the high mountains. This range of K_{HS} values was higher than obtained by Ghamarnia et al. (2011) in western Iran, where it changed from 0.0018 to 0.0042 in a station located in dry and moist sub-humid climates. The annual mean values were 0.01086, 0.01276, and 0.01638 for coast, valley, and mountains, respectively. The estimation for valley is concordant with the 0.01214 found by Almorox et al. (2012) in a dry sub-humid climate.

Accumulated annual ET_o calculated by the calibrated Hargreaves–Samani (HSc) equation is presented in Figure 5. In the coastal area, the stratification showed an ET_o variation between 800 and 1200 mm year^{-1}, which was influenced by low values of solar radiation and extreme temperatures. In the internal rain-fed area (zones which are near to the coastal mountains), there is an increase of solar radiation and temperature range, leading to a rise over 1200 mm year^{-1}. In the central valley ET_o was around 1300 mm year^{-1} and decreases as it approaches to the Andes Mountains. Although, mountain valleys present values around 1000 mm year^{-1}. Above 2000 m above sea level (m.a.s.l) in the Andes Mountains, values reached 700–1000 mm year^{-1}. The observed annual trend is replicated for the monthly scale, where maximum and minimum ET_o values were in summer and winter, respectively.

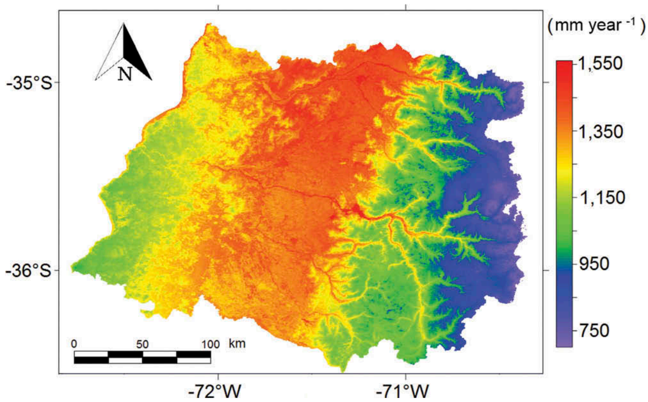

Figure 5. Estimated accumulated annual ET_o by HSc.

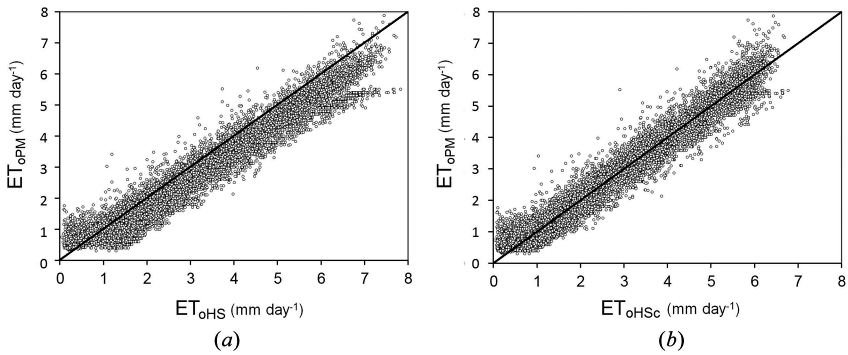

Figure 6. Performance of HS (*a*) and HSc (*b*) for validation.

Table 5. Daily linear regression analysis of original and HSc equation against PM model, HS–PM, and HSc–PM, respectively.

Comparison	b_0	b_1	R^2	p	RMSE (mm day^{-1})	E f	AIC
HS–PM	0.082	0.869	0.947	0.000	0.178	0.932	11,102
HSc–PM	0.146	0.955	0.954	0.000	0.157	0.962	9820

3.3. *Validation*

Analysis showed a HS–PM slope of 0.869 mm mm^{-1}, statistically lower than HSc–PM slope of 0.955 mm mm^{-1} (Table 5). Taking into account this difference, K_{HS} modelling was an effective improvement, based on AIC and RMSE decrease. In Figure 6 it is possible to observe lineal regressions of HS–PM (*a*) and HSc–PM (*b*). R^2 reached over 95% in both cases, but RMSE and Ef were lower for HSc, which showed errors around 0.16 mm day^{-1}, meanwhile HS had values around 0.18 mm day^{-1} like in the literature (Almorox et al. 2012; Thepadia and Martinez 2012; Martinez and Thepadia 2009; Trajkovic and Kolakovic 2009; Droogers and Allen 2002; Hargreaves and Allen 2003). With HSc equation, the MBE and MABE obtained were 0.02 and 0.31 mm day^{-1}, respectively. These values are lower than those obtained by Shahidian et al. (2014), who got an MBE of 0.4 mm day^{-1} in California. Meanwhile at Coronel Dorrego in Argentina under a wet humid climate, Almorox et al. (2012) reported MBE and MABE values of 0.27 and 0.77 mm day^{-1}, respectively. Both studies also considered a calibration process but in a different way than used in this research.

4. Discussion

The average error associated to the ET_o estimation is ranged between 0.4 and 1 mm day^{-1}. This fact makes the local calibration of the K_{HS} coefficient necessary (Hargreaves and Allen 2003). The HS equation assumes that the atmospheric CI is proportional to the square root of the differences between the maximum and minimum daily temperature. Also, the no consideration of wind speed and relative humidity may lead to errors in the ET_o estimation. In this regard, Heydari and Heydari (2013) indicated that HS equation underestimated ET_o under wind speeds conditions below 1.3 m s^{-1}, while Kra (2014) observed an overestimation for a range between 0.5 and 6 m s^{-1}. In this research, all the effects related to relative air humidity and wind speed have been integrated into the K_{HS} coefficient. Furthermore, the study of the effect of the aforementioned climatological variables was not considered here, but it opens a gate to do a deeper analysis of this methodology under Mediterranean conditions.

According to results, the local calibration performed better than the original version of HS equation as reported by Gao et al. (2014). Because of the empiric nature of the HS method, there is usually a need for local calibration (Shahidian et al. 2014). Despite the fact that calibrated parameters such as those indicated in Tables 3 and 4 are specific to the studied areas in this research, which represent one of the main limitations of this type of approaches (Valipour 2014), the calibration methodology could be used as the basis of a pre-calibration for the use in new locations (Shahidian et al. 2014). In this regard, this calibration also has the potential use in the exploration and study of irrigation scheduling in rain-fed lands. A clear example is the southern lands of Chile, where the irrigation is not a common practice, but the arrival of the climate change has developed a new challenge to the growers. Thereby, the availability of a low-input model to know the water consumption at landscape scale would be a good tool for sustainable water management.

5. Conclusion

Regional variability of physiography made the process complex for modelling spatial distribution of climatological variables, thus it was hard to use a classic geostatistical method. Moreover, the number of meteorological stations did not cover the singularities of the territory. GWR showed to be a robust and simple method, constituting itself like a suitable alternative to multiple linear regression and Kriging. Regional ET_o was determined by season of the year, mainly influenced by solar radiation, topography, and distance to Pacific Ocean variations.

The spatial and temporal variability of K_{HS} showed its importance in specific areas, due to the strong dependence on location in the study area. Cluster definition allowed the introduction of affordable parameter values for an extensive knowledge of water requirements. Therefore, spatial calibration of HS equation provided a simple way to estimate ET_o, taking into account the physiography influence on local evaporative demand.

Acknowledgements

This research was partially supported by the Research Program on Adaptation of Agriculture to Climate Change (PIEI A2C2) of the University of Talca and FONDECYT (1130139, 1020202, and 1161809).

Disclosure statement

No potential conflict of interest was reported by the authors.

Funding

This work was supported by the Universidad de Talca, Research Program on Adaptation of Agriculture to Climate Change (A2C2) and FONDECYT [1130139, 1020202, 1161809];

References

Aburto Schweitzer, C. 2007. “Elaboración de un modelo de estimación de la distribución espacial de la radiación solar global mensual para Chile Central.” Ph.D. thesis. Universidad de Chile. Chile.

Allen, R. 1996. “Assessing Integrity of Weather Data for Reference Evapotranspiration Estimation.” *Journal of Irrigation and Drainage Engineering* 122 (April): 97–106. doi:10.1061/(ASCE)0733-9437(1996)122:2(97).

Allen, R. G., L. S. Pereira, D. Raes, and M. Smith. 1998. “Crop Evapotranspiration-Guidelines for Computing Crop Water Requirements – FAO Irrigation and Drainage Paper 56.” *FAO, Rome* 300: 6541.

Almorox, J., V. Elisei, M. E. Aguirre, and M. Commegna. 2012. “Calibration of Hargreaves Model to Estimate Reference Evapotranspiration in Coronel Dorrego, Argentina.” *Revista De La Facultad De Ciencias Agrarias, Universidad Nacional De Cuyo* 44 (1): 101–109.

Ambast, S. K., A. K. Keshari, and A. K. Gosain. 2002. “Satellite Remote Sensing to Support Management of Irrigation Systems: Concepts and Approaches.” *Irrigation and Drainage* 51 (1): 25–39. doi:10.1002/(ISSN)1531-0361.

Brunsdon, C., A. S. Fotheringham, and M. E. Charlton. 1996. “Geographically Weighted Regression: A Method for Exploring Spatial Nonstationarity.” *Geographical Analysis* 28 (4): 281–298. doi:10.1111/j.1538-4632.1996.tb00936.x.

Burnham, K. P., and D. R. Anderson. 1998. *Model Selection and Multimodel Inference: A Practical Information-Theoretic Approach*. New York, NY: Springer-Verlag.

Cammalleri, C., G. Ciraolo, M. Minacapilli, and G. Rallo. 2013. “Evapotranspiration from an Olive Orchard Using Remote Sensing-Based Dual Crop Coefficient Approach.” *Water Resources Management* 27 (14): 4877–4895. doi:10.1007/s11269-013-0444-7.

Castillo, H., and F. Santibañez. 1981. “Evaluación De La Radiación Solar Global Y Luminosidad En Chile, 1: Calibración De Fórmulas Para Estimar Radiación Solar Global Diaria.” *Agricultura Técnica (Chile)* 41 (3): 145–152.

Draper, N. R., and H. Smith. 1981. *Applied Regression Analysis*. New York: John Wiley & Sons.

Droogers, P., and R. G. Allen. 2002. “Estimating Reference Evapotranspiration Under Inaccurate Data Conditions.” *Irrigation and Drainage Systems* 16 (1): 33–45. doi:10.1023/A:1015508322413.

Estévez, J., P. Gavilán, and A. P. García-Marín. 2011. "Data Validation Procedures in Agricultural Meteorology – A Prerequisite for Their Use." *Advances in Science and Research* 6: 141–146. doi:10.5194/asr-6-141-2011.

Gao, X., S. Peng, J. Xu, S. Yang, and W. Wang. 2014. "Proper Methods and Its Calibration for Estimating Reference Evapotranspiration Using Limited Climatic Data in Southwestern China." *Archives of Agronomy and Soil Science* 61 (3): 415–426. doi:10.1080/03650340.2014.933810.

Garreaud, R. D. 2009. "The Andes Climate and Weather." *Advances in Geosciences* 22: 3–11. doi:10.5194/adgeo-22-3-2009.

Ghamarnia, H., V. Rezvani, E. Khodaei, and H. Mirzaei. 2011. "Time and Place Calibration of the Hargreaves Equation for Estimating Monthly Reference Evapotranspiration under Different Climatic Conditions." *Journal of Agricultural Science* 4 (3): 111–122. doi:10.5539/jas.v4n3p111.

Hargreaves, G. H. 1989. "Accuracy of Estimated Reference Crop Evapotranspiration." *Journal of Irrigation and Drainage Engineering* 115 (6): 1000–1007. doi:10.1061/(ASCE)0733-9437(1989)115:6(1000).

Hargreaves, G. H., and R. G. Allen. 2003. "History and Evaluation of Hargreaves Evapotranspiration Equation." *Journal of Irrigation and Drainage Engineering* 129 (1): 53–63. doi:10.1061/(ASCE)0733-9437(2003)129:1(53).

Hargreaves, G. H., and Z. A. Samani. 1982. "Estimating Potential Evapotranspiration." *Journal of the Irrigation and Drainage Division* 108 (3): 225–230.

Hargreaves, G. H., and Z. A. Samani. 1985. "Reference Crop Evapotranspiration from Temperature." *Applied Engineering in Agriculture* 1 (2): 96–99. doi:10.13031/2013.26773.

Heydari, M. M., and M. Heydari. 2013. "Calibration of Hargreaves–Samani Equation for Estimating Reference Evapotranspiration in Semiarid and Arid Regions." *Archives of Agronomy and Soil Science* 60 (5): 695–713. doi:10.1080/03650340.2013.808740.

Higham, D. J. 1992. "Monotonic Piecewise Cubic Interpolation, with Applications to ODE Plotting." *Journal of Computational and Applied Mathematics* 39 (3): 287–294. doi:10.1016/0377-0427(92)90205-C.

Hong, S., V. Lakshmi, and E. Small. 2007. "Relationship between Vegetation Biophysical Properties and Surface Temperature Using Multisensor Satellite Data." *Journal of Climate* 20 (22): 5593–5606. doi:10.1175/2007JCLI1294.1.

Iqbal, M. 1983. *An Introduction to Solar Radiation*. Canada: Academic Press.

Kra, E. 2014. "FAO-56 Penman-Monteith Daily Eto from Linear Regression Calibrated Hargreaves Equation with Wind." *International Journal of Agronomy* 2014: 1–9. doi:10.1155/2014/402809.

Larraín, S. 2006. "El Agua En Chile: Entre Los Derechos Humanos Y Las Reglas Del Mercado." *Polis. Revista Latinoamericana*, 14: 1–20.

Martinez, C., and M. Thepadia. 2009. "Estimating Reference Evapotranspiration with Minimum Data in Florida." *Journal of Irrigation and Drainage Engineering* 136 (7): 494–501. doi:10.1061/(ASCE)IR.1943-4774.0000214.

Martínez-Cob, A. 1996. "Multivariate Geostatistical Analysis of Evapotranspiration and Precipitation in Mountainous Terrain." *Journal of Hydrology* 174 (12): 19–35. doi:10.1016/0022-1694(95)02755-6.

Mendicino, G., and A. Senatore. 2013. "Regionalization of the Hargreaves Coefficient for the Assessment of Distributed Reference Evapotranspiration in Southern Italy." *Journal of Irrigation and Drainage Engineering* 139 (5): 349–362. doi:10.1061/(ASCE)IR.1943-4774.0000547.

Meza, F. 2005. "Variability of Reference Evapotranspiration and Water Demands. Association to ENSO in the Maipo River Basin, Chile." *Global and Planetary Change* 47 (2–4 SPEC. ISS.): 212–220. doi:10.1016/j.gloplacha.2004.10.013.

Meza, F., and E. Varas. 2000. "Estimation of Mean Monthly Solar Global Radiation as a Function of Temperature." *Agricultural and Forest Meteorology* 100 (23): 231–241. doi:10.1016/S0168-1923(99)00090-8.

Miranda-Salas, M., and A. R. Condal. 2003. "Importancia Del Análisis Estadstico Exploratorio En El Proceso De Interpolación Espacial: Caso De Estudio Reserva Forestal Valdivia." *Bosque (Valdivia)* 24 (2): 29–42. doi:10.4067/S0717-92002003000200004.

Morales-Salinas, L. 1997. "Evaluación y zonificación de riesgo de heladas mediante modelización topoclimática." Unpublished doctoral dissertation. Universidad de Concepción. Chile.

Morales-Salinas, L., F. Canessa, C. Mattar, R. Orrego, and F. Matus. 2006. "Caracterización Y Zonificación Edáfica Y Climática De La Región De Coquimbo, Chile." *Revista De La Ciencia Del Suelo Y Nutrición Vegetal* 6 (3): 52–74.

Morales-Salinas, L., G. Castellaro-Galdames, J. C. Parra, J. Espinosa, F. Lang-Tasso, N. Ojeda-Ojeda, and H. Soto-Vera. 2009. "Método De Generación De Cartografa Climática Usando Regresiones Con Pesos Geográficos." *Simiente* 79 (1–2): 74–82.

Novoa, R., S. Villaseca, P. Del Canto, J. Rouanet, C. Sierra, and A. Del Pozo. 1989. *Mapa Agroclimático De Chile*. Santiago: Instituto de Investigaciones Agropectuarias.

Pérez, C. 2004. *Técnicas De Análisis Multivariante De Datos. Aplicaciones Con SPSS*. adrid: Pearson Education.

Qiyao, L., Y. Jingming, and F. Baopu. 1991. "A Method of Agrotopoclimatic Division and Its Practice in China." *International Journal of Climatology* 11 (1): 85–96. doi:10.1002/joc.3370110107.

Rawlings, J. O., S. G. Pantula, and D. A. Dickey. 1998. *Applied Regression Analysis: A Research Tool*. New York, NY: Springer-Verlag.

Raziei, T., and L. S. Pereira. 2013. "Estimation of Eto with Hargreaves-Samani and FAO-PM Temperature Methods for a Wide Range of Climates in Iran." *Agricultural Water Management* 121 (0): 1–18. doi:10.1016/j.agwat.2012.12.019.

Rivano, F., and J. Jara. 2005. "Estimación De La Evapotranspiración De Referencia En La Localidad De Remehue-Osorno, X Región." *Agro Sur* 33 (2): 49–61. doi:10.4206/agrosur.

Sakamoto, Y., M. Ishiguro, and G. Kitagawa. 1986. *Akaike Information Criterion Statistics*. Dordrecht: D. Reidel.

Sánchez, M., and E. Chuvieco. 2000. "Estimación De La Evapotranspiración Del Cultivo De Referencia, ET0, a Partir De Imágenes NOAA-AVHRR." *Revista De Teledetección* 14: 11–21.

Shahidian, S., R. P. Serralheiro, J. R. Serrano, and J. L. Teixeira. 2014. "Seasonal Climate Patterns and Their Influence on Calibration of the Hargreaves-Samani Equation." *Hydrological Sciences Journal* 60 (6): 985–996. doi:10.1080/02626667.2014.938076.

Thepadia, M., and C. Martinez. 2012. "Regional Calibration of Solar Radiation and Reference Evapotranspiration Estimates with Minimal Data in Florida." *Journal of Irrigation and Drainage Engineering* 138 (2): 111–119. doi:10.1061/(ASCE)IR.1943-4774.0000394.

Tomislav, H., H. Sierdsema, A. Radović, and A. Dilo. 2009. "Spatial Prediction of Species Distributions from Occurrence-Only Records: Combining Point Pattern Analysis, {ENFA} and Regression-Kriging." *Ecological Modelling* 220 (24): 3499–3511. doi:10.1016/j.ecolmodel.2009.06.038.

Torres Hernández, A., and R. Vásquez Vásquez. 2013. "Prospección De La Estimación De La Evapotranspiración De Referencia, Bajo Las Condiciones Del Valle De Chaca, Arica-Chile." *Idesia (Arica)* 31 (2): 25–29. doi:10.4067/S0718-34292013000200004.

Trajkovic, S., and S. Kolakovic. 2009. "Estimating Reference Evapotranspiration Using Limited Weather Data." *Journal of Irrigation and Drainage Engineering* 135 (4): 443–449. doi:10.1061/(ASCE)IR.1943-4774.0000094.

Tucker, C. J. 1979. "Red and Photographic Infrared Linear Combinations for Monitoring Vegetation." *Remote Sensing of Environment* 8 (2): 127–150. doi:10.1016/0034-4257(79)90013-0.

Uribe, J. M., R. Cabrera, A. De La Fuente, and M. Paneque. 2012. *Atlas Bioclimático De Chile*. Santiago: Universidad de Chile.

Valipour, M. 2014. "Use of Average Data of 181 Synoptic Stations for Estimation of Reference Crop Evapotranspiration by Temperature-Based Methods." *Water Resources Management* 28 (12): 4237–4255. doi:10.1007/s11269-014-0741-9.

Valipour, M. 2015a. "Comparative Evaluation of Radiation-Based Methods for Estimation of Potential Evapotranspiration." *Journal of Hydrologic Engineering* 20 (5): 1–14. doi:10.1061/(ASCE)HE.1943-5584.0001066.

Valipour, M. 2015b. "Evaluation of Radiation Methods to Study Potential Evapotranspiration of 31 Provinces." *Meteorology and Atmospheric Physics* 127 (3): 289–303. doi:10.1007/s00703-014-0351-3.

Valipour, M. 2015c. "Importance of Solar Radiation, Temperature, Relative Humidity, and Wind Speed for Calculation of Reference Evapotranspiration." *Archives of Agronomy and Soil Science* 61 (2): 239–255.

Valipour, M. 2015d. "Investigation of Valiantzas' Evapotranspiration Equation in Iran." *Theoretical and Applied Climatology* 121 (1): 267–278. doi:10.1007/s00704-014-1240-x.

Valipour, M. 2015e. "Study of Different Climatic Conditions to Assess the Role of Solar Radiation in Reference Crop Evapotranspiration Equations." *Archives of Agronomy and Soil Science* 61 (5): 679–694. doi:10.1080/03650340.2014.941823.

Valipour, M. 2015f. "Temperature Analysis of Reference Evapotranspiration Models." *Meteorological Applications* 22 (3): 385–394. doi:10.1002/met.1465.

Valipour, M., and S. Eslamian. 2014. "Analysis of Potential Evapotranspiration Using 11 Modified Temperature-Based Models." *International Journal of Hydrology Science and Technology* 4 (3): 192–207. doi:10.1504/IJHST.2014.067733.

Vermote, E. F., and S. Y. Kotchenova. 2011. *MOD09 (Surface Reflectance) Users Guide*. Greenbelt: MODIS Land Surface Reflectance Science Computing Facility.

Vicente Serrano, S. M., S. Sánchez, and J. M. Cuadrat. 2003. "Comparative Analysis of Interpolation Methods in the Middle Ebro Valley (Spain): Application to Annual Precipitation and Temperature." *Climate Research* 24 (2): 161–180. doi:10.3354/cr024161.

Westerhoff, R. S. 2015. "Using Uncertainty of Penman and Penman Monteith Methods in Combined Satellite and Ground-Based Evapotranspiration Estimates." *Remote Sensing of Environment* 169: 102–112. doi:10.1016/j.rse.2015.07.021.